Enhancing Neurofibroma Segmentation in Whole-Body MRI: Leveraging an Anatomy-Informed Approach

Georgii Kolokolnikov[1,2] G.KOLOKOLNIKOV@UKE.DE
Marie-Lena Schmalhofer[3] M.SCHMALHOFER@UKE.DE
Inka Ristow[3] I.RISTOW@UKE.DE
René Werner[1,2] R.WERNER@UKE.DE
[1] *Institute for Applied Medical Informatics, University Medical Center Hamburg-Eppendorf*
[2] *Institute for Computational Neuroscience, University Medical Center Hamburg-Eppendorf*
[3] *Department of Diagnostic and Interventional Radiology and Nuclear Medicine, University Medical Center Hamburg-Eppendorf*

Editors: Accepted for publication at MIDL 2024

Abstract

This study presents an anatomy-informed segmentation approach for neurofibroma in fat-suppressed T2-weighted whole-body MRI (WB-MRI). By adapting TotalSegmentator for WB-MRI segmentation and employing dedicated Dynamic UNet models across four anatomical zones, we achieved improvements of 20% in terms of the Dice coefficient on a test set. The proposed method promises to streamline neurofibroma segmentation, emphasizing future integration into interactive workflows.

Keywords: Neurofibroma, whole-body MRI, deep learning, medical image segmentation, anatomy-informed approach, TotalSegmentator.

1. Introduction

Neurofibromas (NFs), associated with the genetic disorder neurofibromatosis type 1 (NF1), manifest as tumors along nerves in the skin and deeper soft tissues (Lammert et al., 2005). Monitoring NF1 patients is critical due to the potential for malignancy with a high tumor burden being a risk factor for malignant transformation (Korf, 1999). Whole-body MRI (WB-MRI) is an important clinical feature in NF diagnosis (Legius et al., 2021), yet challenges in manual tumor quantification (Kollmann et al., 2020) and the subjectiveness of human observers prompt a need for enhanced methods. NF segmentation, vital for the analysis, is time-intensive and challenging, with manual segmentation taking up to five hours per patient and state-of-the-art automatic methods like nnU-Net showing only 25% accuracy (Zhang et al., 2022). While semi-automatic interactive methods (Diaz-Pinto et al., 2022) improve accuracy, they still demand significant manual intervention in case of high tumor load. Improved automatic pre-segmentation in addition to the interactive pipeline alleviates the manual effort.

We propose an anatomy-informed approach to the automatic pre-segmentation of NF in WB-MRI. As it was reported in (Zhang et al., 2022), a default nnU-Net pipeline shows a low performance on this task. Hence, we leverage the acquisition of anatomical information from accompanying T1-weighted (T1w) data. Our contributions are: 1) establishing a pipeline for anatomy segmentation based on the adaptation of the TotalSegmentator; 2) inclusion of the anatomical information in the NF segmentation; 3) anatomical zone based NF segmentation.

2. Materials and Methods

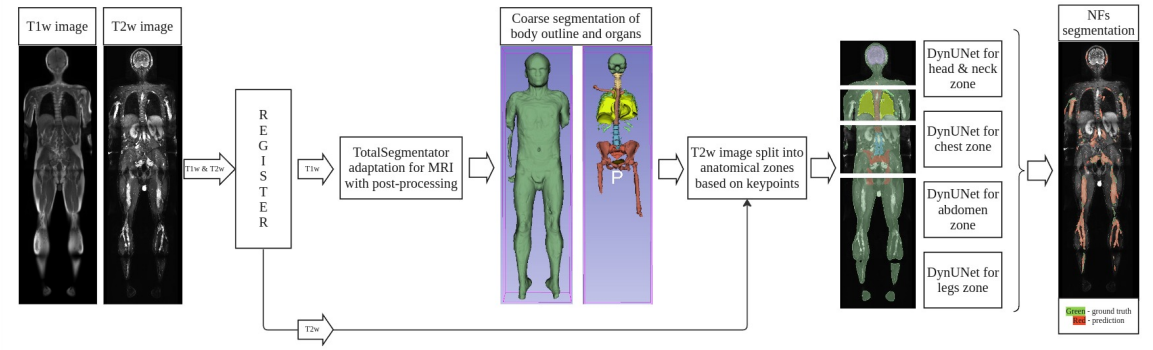

Figure 1: Anatomy-informed neurofibromas (NFs) segmentation pipeline. T1w and T2w MRIs are registered. T1w is segmented with the adapted TotalSegmentator to get anatomical masks. T2w is split into anatomical zones. Each zone is segmented with a dedicated DynUnet to get respective NFs masks. The NFs masks are stitched together to form the final segmentation mask.

Dataset. Single-center data was acquired at the University Medical Center Hamburg-Eppendorf. The dataset contained T1w and T2-weighted (T2w) fat-suppressed WB-MRIs of 60 patients covering a period of 14 years (2006 - 2020). NF tumors in the dataset were manually segmented with ITK-SNAP 3.8.0 (Yushkevich et al., 2006) by two radiologists (I.R. and M.-L. S.). The WB-MRIs were randomly split on a patient level into train (48 patients, 70 MRIs, median tumor burden 319 ml), validation (6 patients, 12 MRIs, median tumor burden 413 ml), and test subset (6 patients, 11 MRIs, median tumor burden 602 ml). The dataset underwent spacing alignment, Gaussian smoothing, and intensity scaling.

Anatomy-informed segmentation. NFs show a predisposition for the head/neck, trunk, and extremities locations (Staser et al., 2012). According to the initial data analysis, the appearance of NFs depends on their localization within a body. For example, NFs located in the legs can look similar to blood vessels, and those in the neck can resemble lymph nodes. Given varied appearances of NFs across anatomical zones (Staser et al., 2012), providing location of organs and considering the zones separately could enhance segmentation accuracy. We used T1w WB-MRI to capture anatomical structures, since it provides high contrast between fat and water-containing tissues. For identifying NFs, we used fat-suppressed T2w WB-MRI, which is more sensitive to a fluid content (Ahlawat et al., 2016). T1w and T2w WB-MRIs were rigidly registered to compensate for a patient positioning (Figure 1). We trained the TotalSegmentator (Wasserthal et al., 2023) using an unsupervised domain adaptation method to adapt it to the highly-anisotropic T1w WB-MRI data following (Weihsbach et al., 2023). The adapted model segmented key anatomical features in T1w WB-MRI, including body surface and internal organs, which were refined by removing inaccuracies through connected component analysis. The T2w WB-MRI was divided into four anatomical zones (head-neck, chest, abdomen, and legs) based on the landmarks identified from the anatomy segmentation. By dividing the body into these

zones, we tailored the analysis to each region, accommodating the appearance of tumors in different body parts. We trained four Dynamic UNets (DynUNets) with anisotropic kernels and strides suited for each zone. The segmentation was performed patch-wise. An anatomy segmentation mask was passed as the second channel for each DynUNet. Segmentations of NF for each zone were stitched together to form the whole-body NF mask. Since the assessment of internal tumor load is of major importance for physicians, we applied masking with a morphologically eroded body outline to focus only on the deep soft tissue NFs and to exclude superficial cutaneous NF that do not tend to undergo malignant transformations.

3. Results

To evaluate the effect of the anatomy-informed approach (Table 1), we compared the baseline method, whole-body NF segmentation with DynUNet (patch size 128x128x32) without any anatomical information included (denoted as WB), the WB method with anatomy masks given as the second channel (WBA), an anatomical zone based segmentation with a set of DynUNet models described above (ZB), and the ZB method with anatomy masks given as the second channel (ZBA). Additionally, we checked the effect of masking the segmentation with an eroded body outline (removed 1 cm below the skin surface). Two metrics were used: Dice similarity coefficient (DSC) and volume overlap error (VOE).

Table 1: Comparison of the performance of the segmentation pipelines.

Segmentation	**Validation DSC (↑)**	**Validation VOE (↓)**	**Test DSC (↑)**	**Test VOE (↓)**
WB (baseline)	0.34 ± 0.19	0.78 ± 0.15	0.32 ± 0.08	0.79 ± 0.07
WB + masking	0.34 ± 0.19	0.77 ± 0.15	0.35 ± 0.09	0.78 ± 0.08
WBA	0.39 ± 0.15	0.74 ± 0.12	0.34 ± 0.08	0.78 ± 0.07
WBA + masking	0.39 ± 0.14	0.74 ± 0.12	0.37 ± 0.09	0.77 ± 0.08
ZB	0.44 ± 0.15	0.71 ± 0.16	0.51 ± 0.07	0.65 ± 0.07
ZB + masking	0.43 ± 0.16	0.69 ± 0.19	0.54 ± 0.07	0.63 ± 0.07
ZBA	0.43 ± 0.16	0.70 ± 0.15	0.53 ± 0.06	0.64 ± 0.05
ZBA + masking	0.43 ± 0.19	0.71 ± 0.17	0.54 ± 0.06	0.62 ± 0.06

Our findings for the baseline aligned with (Zhang et al., 2022) that showed low DSC of 0.25 for the nnU-Net. We observed high performance variability among the cases with lower tumor burden. Segmenting NFs by anatomical zones enhanced accuracy, particularly for the test cases with greater tumor burden (20% increase of DSC). Employing anatomy masks showed only a marginal improvement. We also evaluated the average number of user interactions required to reach a DSC of 0.6, starting from the pre-segmentation masks. When employing the ZBA masks, we observed a decrease in the average number of interactions by 30% (59 interactions), compared to the baseline (80 interactions).

4. Conclusion

Our study introduced an anatomy-informed pipeline for NF segmentation in WB-MRI, enhancing preliminary delineation accuracy. By incorporating anatomical information and segmenting based on the specific body zones, we achieved a substantial improvement in the Dice similarity coefficient, highlighting the method's efficacy. Future efforts will focus on integrating this pipeline into a semi-automated workflow to streamline NF segmentation.

Acknowledgments

This work was supported by DFG grant (DFG SPP 2177), project number 515277218.

References

Shivani Ahlawat, Laura M. Fayad, Muhammad Shayan Khan, Miriam A. Bredella, Gordon J. Harris, D. Gareth Evans, et al. Current whole-body MRI applications in the neurofibromatoses: NF1, NF2, and schwannomatosis. *Neurology*, 87(7_Supplement_1), August 2016. ISSN 0028-3878, 1526-632X. doi: 10.1212/WNL.0000000000002929. URL https://www.neurology.org/doi/10.1212/WNL.0000000000002929.

Andres Diaz-Pinto, Pritesh Mehta, Sachidanand Alle, Muhammad Asad, Richard Brown, Vishwesh Nath, Alvin Ihsani, Michela Antonelli, Daniel Palkovics, Csaba Pinter, Ron Alkalay, Steve Pieper, Holger R. Roth, Daguang Xu, Prerna Dogra, Tom Vercauteren, Andrew Feng, Abood Quraini, Sebastien Ourselin, and M. Jorge Cardoso. DeepEdit: Deep Editable Learning for Interactive Segmentation of 3D Medical Images. In Hien V. Nguyen, Sharon X. Huang, and Yuan Xue, editors, *Data Augmentation, Labelling, and Imperfections*, pages 11–21, Cham, 2022. Springer Nature Switzerland. ISBN 9783031170270. doi: 10.1007/978-3-031-17027-0_2.

Philipp Kollmann, Victor-Felix Mautner, Johannes Koeppen, Ralph Wenzel, Jan M. Friedman, Johannes Salamon, and Said Farschtschi. MRI based volumetric measurements of vestibular schwannomas in patients with neurofibromatosis type 2: comparison of three different software tools. *Scientific Reports*, 10(1):11541, July 2020. ISSN 2045-2322. doi: 10.1038/s41598-020-68489-y. URL https://www.nature.com/articles/s41598-020-68489-y.

Bruce R. Korf. Plexiform neurofibromas. *American Journal of Medical Genetics*, 89(1):31–37, March 1999. ISSN 0148-7299, 1096-8628. doi: 10.1002/(SICI)1096-8628(19990326)89:1⟨31::AID-AJMG7⟩3.0.CO;2-W. URL https://onlinelibrary.wiley.com/doi/10.1002/(SICI)1096-8628(19990326)89:1<31::AID-AJMG7>3.0.CO;2-W.

Marga Lammert, Jan M. Friedman, Lan Kluwe, and Victor F. Mautner. Prevalence of Neurofibromatosis 1 in German Children at Elementary School Enrollment. *Archives of Dermatology*, 141(1):71–74, January 2005. ISSN 0003-987X. doi: 10.1001/archderm.141.1.71. URL https://doi.org/10.1001/archderm.141.1.71.

Eric Legius, Ludwine Messiaen, Pierre Wolkenstein, Patrice Pancza, Robert A. Avery, Yemima Berman, et al. Revised diagnostic criteria for neurofibromatosis type 1 and Legius syndrome: an international consensus recommendation. *Genetics in Medicine*, 23(8):1506–1513, August 2021. ISSN 10983600. doi: 10.1038/s41436-021-01170-5. URL https://linkinghub.elsevier.com/retrieve/pii/S1098360021050747.

Karl Staser, Feng-Chun Yang, and D. Wade Clapp. Pathogenesis of Plexiform Neurofibroma: Tumor-Stromal/Hematopoietic Interactions in Tumor Progression. *Annual Review of*

Pathology: Mechanisms of Disease, 7(1):469–495, February 2012. ISSN 1553-4006, 1553-4014. doi: 10.1146/annurev-pathol-011811-132441. URL https://www.annualreviews.org/doi/10.1146/annurev-pathol-011811-132441.

Jakob Wasserthal, Hanns-Christian Breit, Manfred T. Meyer, Maurice Pradella, Daniel Hinck, Alexander W. Sauter, Tobias Heye, Daniel T. Boll, Joshy Cyriac, Shan Yang, Michael Bach, and Martin Segeroth. TotalSegmentator: Robust Segmentation of 104 Anatomic Structures in CT Images. *Radiology: Artificial Intelligence*, 5(5):e230024, September 2023. ISSN 2638-6100. doi: 10.1148/ryai.230024. URL http://pubs.rsna.org/doi/10.1148/ryai.230024.

Christian Weihsbach, Christian N. Kruse, Alexander Bigalke, and Mattias P. Heinrich. DG-TTA: Out-of-domain medical image segmentation through Domain Generalization and Test-Time Adaptation, December 2023. URL http://arxiv.org/abs/2312.06275. arXiv:2312.06275 [cs].

Paul A. Yushkevich, Joseph Piven, Heather Cody Hazlett, Rachel Gimpel Smith, Sean Ho, James C. Gee, and Guido Gerig. User-guided 3D active contour segmentation of anatomical structures: Significantly improved efficiency and reliability. *NeuroImage*, 31 (3):1116–1128, July 2006. ISSN 1053-8119. doi: 10.1016/j.neuroimage.2006.01.015. URL https://www.sciencedirect.com/science/article/pii/S1053811906000632.

Jian-Wei Zhang, Wei Chen, K. Ina Ly, Xubin Zhang, Fan Yan, Justin Jordan, Gordon Harris, Scott Plotkin, Pengyi Hao, and Wenli Cai. DINs: Deep Interactive Networks for Neurofibroma Segmentation in Neurofibromatosis Type 1 on Whole-Body MRI. *IEEE Journal of Biomedical and Health Informatics*, 26(2):786–797, February 2022. ISSN 2168-2208. doi: 10.1109/JBHI.2021.3087735. URL https://ieeexplore.ieee.org/abstract/document/9449950.